Evidence for Solitons in Hydrogen-Bonded Systems

Eric S. Nylund
Department of Chemistry, B-040, University of California, San Diego, La Jolla, California 92093

George P. Tsironis[a]
Fermi National Accelerator Laboratory, P.O. Box 500, MS 345, Batavia, Illinois 60510
(Received 9 July 1990)

Langevin-type finite-temperature simulations show that soliton mobility in hydrogen-bonded chains is a nonmonotonic function of temperature. In the temperature range of 170–240 K, soliton mobility initially increases, reaches a maximum at approximately 190 K, subsequently decreases to a minimum at approximately 210 K, and then increases again. This behavior is in qualitative agreement with experimental data for ice crystals in the same temperature range.

PACS numbers: 66.30.Dn, 05.40.+j, 87.22.Fy

There has recently been substantial interest in the study of possible collective proton motion in hydrogen-bonded systems.[1-12] This interest has been largely motivated by the large number of organic as well as inorganic substances that form chains, networks, as well as solids utilizing hydrogen-bonding mechanisms. Ice and hydrogen halides are the best known examples of inorganic hydrogen-bonded solids,[5,6,13] whereas proteins, DNA, and other biological macromolecules are examples of organic hydrogen-bonded materials.[14,15] It is a well established fact that protons are the dominant charge carriers in hydrogen-bonded chains and that they move more efficiently in the direction of hydrogen bonds than in alternative directions.[13] This efficiency in proton transport has been associated in the case of proton transfer across cellular membranes (proton pump) with possible coherence features in the proton motion.[14,15] The cooperative proton dynamics in the networks can be directly attributed to the proton-proton interaction as well as to the nonlinear nature of the hydrogen bond. In the case of ice, for instance, a proton bonds covalently with an oxygen atom (bond length approximately 1.0 Å) and forms a hydrogen bond with the adjacent oxygen atom (bond length approximately 1.7 Å). Because of the symmetry of an isolated oxygen-proton-oxygen complex the proton may also form a hydrogen bond with the first oxygen and bond covalently to the second one. As a result, the effective proton potential has two symmetric equilibrium positions separated by a potential barrier, i.e., has the form of a double well. The properties of the proton potential and the proton-proton interaction lead very naturally to the association of possible coherence in proton motion with the concept of topological solitons.[1] A number of quasi-one-dimensional nonlinear models have been proposed in order to study coherence of proton motion in hydrogen-bonded chains.[1,3,8,9,12] In the present Letter we use a simple model for ionic defects that captures all the essential physics and we report temperature-dependent mobility results.

The nonlinear model consists of an alternating sequence of proton and ion masses [Fig. 1(a)]. The protons (dark circles) are placed in double-well potentials [Fig. 1(b)] of the form

$$V(u_j)=\varepsilon_0(1-u_j^2/b^2)^2, \tag{1}$$

where u_j is the displacement of the jth proton, ε_0 is the barrier height of the potential well, and b is the distance from the local minima to the maximum of the proton potential.

The proton motion in the chain is governed by the Hamiltonian

$$H_{\text{proton}}=\sum_j\left\{\frac{m}{2}\left[\frac{du_j}{dt}\right]^2+\tfrac{1}{2}m\omega_1^2(u_{j+1}-u_j)^2+V(u_j)\right\}, \tag{2}$$

where m is the mass of the proton and ω_1 is the frequency of acoustic (proton) vibrations. The ion chain is de-

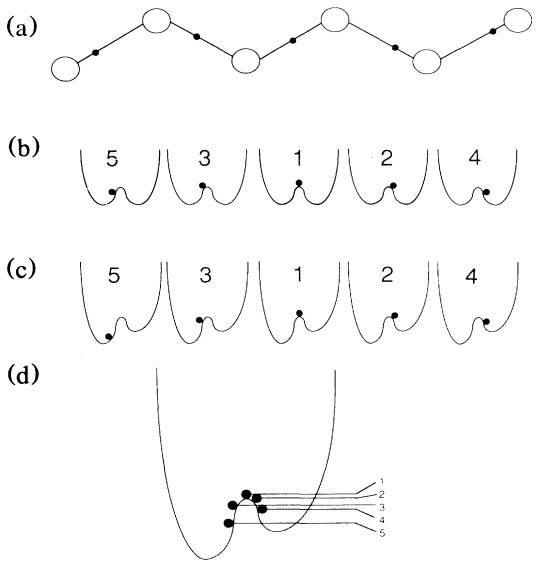

FIG. 1. The proton potentials in a quasi-one-dimensional hydrogen-bonded chain (a) are well approximated by symmetric double wells (b). An external (negative) electric field effectively breaks the symmetry of the hydrogen-bond potential (c), and protons adjacent to the top of the barrier have different potential energies (d).

© 1991 The American Physical Society

scribed by the Hamiltonian

$$H_{\text{ion}}=\sum_j\left\{\frac{M}{2}\left(\frac{dw_j}{dt}\right)^2+\tfrac{1}{2}M\Omega_1^2(w_{j+1}-w_j)^2+\tfrac{1}{2}M\Omega_0^2w_j^2\right\}, \quad (3)$$

where M is the mass of the oxygen ion, Ω_0 is the frequency of a pseudo-optical branch, and Ω_1 is the acoustic ion frequency. Protons and ions interact with

$$H_{\text{interaction}}=\sum_j\tfrac{1}{2}\chi w_j(u_j^2-b^2), \quad (4)$$

where χ is the strength of the interaction. As a result of the interaction term, the double-well proton potential is dynamically altered by the motion of the ions. For large ion displacements the effective barrier height is reduced substantially, thereby permitting ion-assisted proton motion.

The Hamiltonian for the entire chain is $H=H_{\text{proton}}+H_{\text{ion}}+H_{\text{interaction}}$. Analytical solutions for the discrete model can only be obtained in the continuum limit for $\Omega_0=0$, and only for a characteristic velocity v_0 (ion sound velocity). These solutions describe a hyperbolic-tangent kink-shaped proton soliton that is producing and carrying with it a sech^2-shaped ion deformation.[1] For $v\neq v_0$ the solutions do not change substantially.[4] In the case of ice crystals the dressed kinks and antikinks represent OH^- and H_3O^+ defects, respectively.[1,4]

In order to study the defect motion at finite temperatures the hydrogen-bonded chain is placed in a heat reservoir[16] and a constant electric field (E) is turned on. The electric field effectively breaks the symmetry of the proton double well [Fig. 1(c)]. The proton and ion equations of motion are then

$$\frac{d^2u_j}{dt^2}=\omega_1^2(u_{j+1}+u_{j-1}-2u_j)+\frac{4\varepsilon_0}{mb^2}u_j\left(1-\frac{u_j^2}{b^2}\right)-\frac{\chi}{m}w_ju_j+\frac{eE}{m}, \quad (5)$$

$$\frac{d^2w_j}{dt^2}+\gamma\frac{dw_j}{dt}=\Omega_1^2(w_{j+1}+w_{j-1}-2w_j)-\Omega_0^2w_j-\frac{\chi}{2M}(u_j^2-b^2)+\frac{f_n(t)}{M}, \quad (6)$$

where γ is a damping coefficient and $f_n(t)$ represents a Langevin-type δ-correlated Gaussian stochastic force that acts on the nth ion:

$$\langle f_n(t)f_{n'}(t')\rangle=2k_BTM\gamma\delta_{n,n'}\delta(t-t'). \quad (7)$$

We cast the equations of motion (5) and (6) in dimensionless form by choosing the time unit equal to 1.0214×10^{-14} s (frequency unit of 0.9787×10^{-14} s^{-1}), mass unit equal to the proton mass, and unit of length equal to 1.0 Å. We then integrate them numerically using the fourth-order Runge-Kutta scheme. We typically use a chain with 100 unit cells. The values of the physical parameters are comparable with experimental data as well as other work in this field.[4,9,12] We take $\varepsilon_0=2.0$ eV, $b=1.0$ Å, $a=5.0$ Å, $m=1.0$ amu, $M=17.0$ amu, $\omega_1=5.87\times10^{-14}$ s^{-1}, $\Omega_0=1.80\times10^{-13}$ s^{-1}, $\Omega_1=5.87\times10^{-13}$ s^{-1}, $\chi=0.10$ eV/Å^3 with the integration time step dt typically taken equal to 0.05 time unit. Since time discretization affects the properties of the Langevin forces in the numerical simulations, we use an ensemble of Gaussian forces f_n with variance equal to

$$\sigma=(k_BTM\gamma/dt)^{1/2}. \quad (8)$$

This choice of Gaussian width is compatible with the fluctuation-dissipation theorem and time discretization.[17]

To ensure that the chain is at temperature T we use the following procedure. Initially the chain is interacting with the Langevin bath at temperature T with no soliton present. We monitor the total kinetic energy of the ions and protons in the chain, which after some initial fluctuations relaxes to and maintains an average value equal to kT per unit cell in accordance with the equipartition theorem. Subsequently we use the analytic soliton solutions[1] and introduce a soliton in the lattice by modifying the displacements of a small number of protons and ions around the defect center. We monitor the defect motion over a temperature range of 170–240 K and fields in the range of 100–200 kV/cm.[18] The kink soliton accompanied by the ion deformation accelerates initially while the temperature fluctuations produce small random deviations in the proton and ion displacements. We register the defect velocity at longer times when the kink-deformation complex reaches a steady state moving with a constant velocity.

In Fig. 2 we present the result of our numerical evaluation of the defect mobility. We plot the terminal defect velocities as a function of inverse temperature for two different field values. We note that as the temperature increases the defect mobility rises and peaks around 190 K. Subsequently it drops, reaches a minimum at approximately 210 K, and then rises again. This behavior is clear for these two field values presented here even though there are differences in the details of the curves. The nonmonotonic up-down-up tendency for this range of temperatures seems to be a generic feature in the temperature dependence of the soliton mobility and observed for other field values (Fig. 3) and different barrier heights.[19]

The most distinct feature of the mobility-temperature plots is the presence of two transition temperatures $T_{\max}=190$ K and $T_{\min}=210$ K, where the defect velocity reaches a maximum and minimum, respectively. Upon comparing the simulated data with polycrystalline ice data[13,20] (Fig. 2, inset) we observe in the latter the same qualitative behavior: temperature-assisted mobility at small temperatures and high temperatures with a very distinct drop in the intermediate region. In addition to

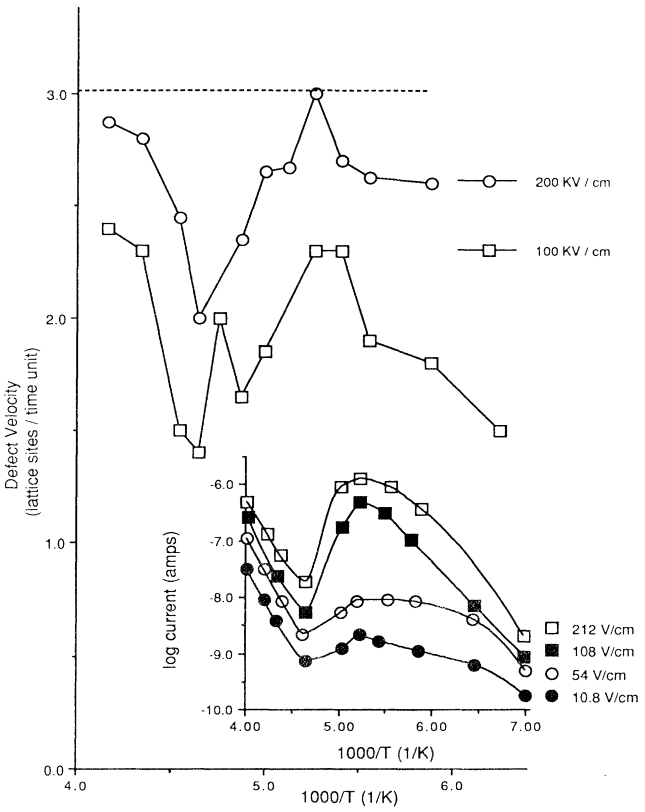

FIG. 2. Nonlinear defect velocity as a function of inverse temperature for two field values. Transition temperatures occur at $T_{max}=190$ K and $T_{min}=210$ K. The dotted line represents the ion sound velocity v_0. Inset: Experimental data for current as a function of inverse temperature for ice crystals (Refs. 13 and 20).

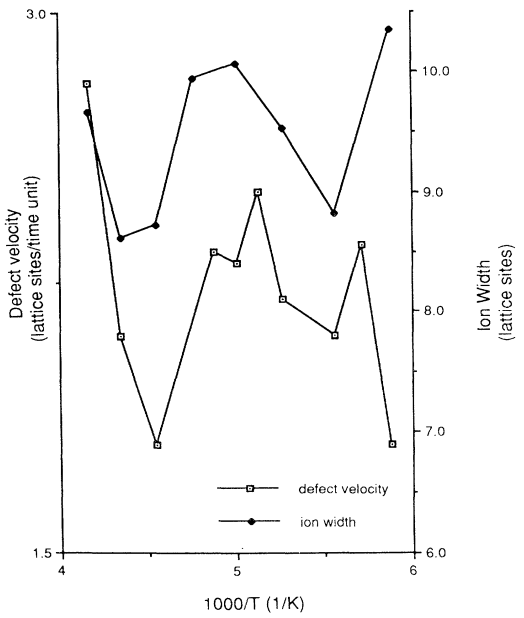

FIG. 3. Nonlinear defect velocity as a function of inverse temperature for 150 kV/cm field and the corresponding (ion) defect width as a function of inverse temperature. The increase of the defect width at intermediate and large temperatures signifies larger ion and proton participation in the defect motion.

the qualitative similarity of the conductivity (experimental data) and velocity (nonlinear model) temperature dependences, the most remarkable feature is that the transition temperatures of the experimental and simulated data coincide.

The temperature dependence of the defect velocity can be directly attributed to the nonlinear nature of the proton potential in the context of the nonlinear model. In the absence of a field the proton defect is symmetric around a central proton which lies at the top of the potential barrier [proton 1 in Fig. 1(b)]. Adjacent to the defect center there are pairs of protons that lie lower on the potential surface with equal potential energies [protons 2,3 and 4,5, etc., in Fig. 1(b)]. When a field is applied these protons have a preferred direction, viz. the direction of the field. Since the symmetry of the potential is effectively broken, the proton pairs adjacent to the center of the defect from either side will now have unequal potential energies. For instance, proton 2, which is next to the center of the defect in the direction opposite to the field [Fig. 1(c)], is now closer to the top of its local barrier than proton 3. The ranking of the position of the protons from the top of the barrier goes from one side of the center of the defect to the other.

When thermal motion is introduced, an entire spectrum of Gaussian random displacements with a given temperature-dependent width are imposed upon the ion chain. In the absence of a field the protons that constitute the defect are executing locally a random walk. At small temperatures, the proton which lies closest to the top of the potential-energy barrier (proton 2) has a more favorable mechanism to cross over when the field is turned on. This mechanism becomes increasingly likely as temperature increases. Thermal fluctuations are just as likely to push the proton towards the barrier as they are to pull it towards the bottom of the well. On the average, however, defect velocity increases because proton 2 is more likely to cross over than proton 3 [Fig. 1(d)]. As the temperature continues to increase a second mechanism in the dynamics of the proton chain is possible due to the larger ion displacements. Proton 3 can now cross the barrier more frequently and because of this the defect motion is hindered. This is manifested in the simulations by the decrease of the defect velocity with temperature. This effect of random ion motion helping and hindering the defect velocity is repeated also at higher temperatures with protons further distant from the defect center. The increase in soliton velocity for temperature larger than $T_{min}=210$ K is directly attributed to the influence of the outer-layer protons, viz. the protons that are further from the centroid of the defect. These outer-layer protons cannot cross the potential bar-

rier solely due to thermal fluctuations in this temperature range. They can, however, transmit their additional thermal energy to protons closer to the top of the barrier which in turn can now cross over. In this temperature range, due to the asymmetry in the potential well, proton 4 in Figs. 1(c) and 1(d) has on the average larger indirect impact to the motion of the soliton than proton 5 and as a result there is an indirect velocity assistance by these outer-layer protons.

In Fig. 3 we show the ion defect width as a function of $1/T$ for a field value equal to 150 kV/cm and the corresponding temperature-dependent velocity dependence for the same field. In order to exclude contributions due to purely thermal distortions, we define the defect width in such a way as to include those ions whose displacement lies within 65% of the maximum ion deformation caused by the presence of the kink in the proton sublattice. We note that the defect width, typified here by the average ion defect width, is a sensitive function of the temperature. The peak in the width size in between the transition temperatures $T_{\min}$ and $T_{\max}$ signifies that outer-layer protons and ions participate more in the temperature-induced defect motion, in accordance with the previous physical explanation.

In this study we obtained numerically a very distinct nonmonotonic temperature dependence for the soliton mobility in hydrogen-bonded chains which we attribute to a competition between field-induced biased proton motion and temperature fluctuations.[21] Upon comparing it with available conductivity data for ice we found remarkable quantitative agreement in the transition-temperature values and qualitative similarity in the corresponding conductivity and defect-velocity curves. There are, however, various limitations to this comparison. In particular, the difference between the conductivity value at $T_{\max}$ and $T_{\min}$ is much more pronounced in the ice data than in the simulated data. This difference can be attributed to various factors, such as the particular choice of electric-field values,[18] the values of the parameters in the model such as the barrier height ε_0, the nonlinear coupling parameter χ, and the spring constants, the absence from the model of many-body effects, and most importantly the real three-dimensional nature of ice. Because of the latter, other conductivity channels, such as orientational defects,[13] are available to the real hydrogen-bonded system and the temperature effects are compounded. Furthermore, thermally activated defect creation which dominates in ice in the high-temperature regime[13] is not included in the present one-soliton model. Even with these limitations we believe that the striking similarity between simulations and ice data provides evidence for the compatibility of the soliton picture with the defects in a hydrogen-bonded network.

We thank K. Lindenberg, St. Pnevmatikos, D. W. Brown, and A. Zolotaryuk for valuable discussions. One of us (E.S.N.) acknowledges partial support of NSF Grant No. DMR 86-19650-A1.

[a]Present and permanent address: Physics Department, P.O. Box 5368, University of North Texas, Denton, TX 76203.

[1]V. Ya. Antonchenko, A. S. Davydov, and A. V. Zolotaryuk, Phys. Status Solidi (b) **115**, 631 (1983).

[2]A. V. Zolotaryuk, K. H. Spatscheck, and E. W. Laedke, Phys. Lett. **101A**, 517 (1984); E. W. Laedke, K. H. Spatschek, M. W. Wilkens, Jr., and A. V. Zolotaryuk, Phys. Rev. A **32**, 1161 (1985).

[3]A. V. Zolotaryuk, in *Biophysical Aspects of Cancer*, edited by J. Fiala and J. Prokorny (Charles Univ. Press, Prague, 1987).

[4]M. Peyrard, St. Pnevmatikos, and N. Flytzanis, Phys. Rev. A **36**, 903 (1987).

[5]M. Springborg, Phys. Rev. Lett. **59**, 2287 (1987); Phys. Rev. B **38**, 1438 (1988).

[6]R. W. Jansen, R. Bertocini, D. A. Pinnick, A. I. Katz, R. C. Hanson, O. F. Sankey, and M. O'Keeffe, Phys. Rev. B **35**, 9830 (1987).

[7]J. Halding and P. S. Lomdahl, Phys. Rev. A **37**, 2608 (1988).

[8]St. Pnevmatikos, Phys. Rev. Lett. **60**, 1534 (1988).

[9]G. P. Tsironis and St. Pnevmatikos, Phys. Rev. B **39**, 7161 (1989).

[10]D. Hochstrasser, H. Büttner, H. Desfoutaines, and M. Peyrard, Phys. Rev. A **38**, 5332 (1988).

[11]St. Pnevmatikos, G. P. Tsironis, and A. V. Zolotaryuk, J. Mol. Liquids **41**, 85 (1989), and references therein.

[12]A. Zolotaryuk and St. Pnevmatikos, Phys. Lett. A **143**, 233 (1990).

[13]P. B. Hobbs, *Ice Physics* (Clarendon, Oxford, 1974).

[14]E. W. Knapp, K. Schulten, and Z. Schulten, Chem. Phys. **46**, 215 (1980); J. F. Nagle, M. Mille, and H. J. Morowitz, J. Chem. Phys. **72**, 298 (1980); J. F. Nagle and H. J. Morowitz, Proc. Natl. Acad. Sci. U.S.A. **75**, 298 (1978).

[15]J. F. Nagle and S. Tristam-Nagle, J. Membrane Biol. **74**, 1 (1983).

[16]P. S. Lomdahl and W. C. Kerr, Phys. Rev. Lett. **55**, 1235 (1985).

[17]E. Helfand, Bell Syst. Tech. J. **58**, 2289 (1979); H. S. Greenside and E. Helfand, Bell Syst. Tech. J. **60**, 1927 (1981); L. Ramirez-Piscina, J. M. Sancho, F. J. de la Rubia, K. Lindenberg, and G. P. Tsironis, Phys. Rev. A **40**, 2120 (1989).

[18]These field values are in the biologically interesting range (Refs. 14 and 15) and also much smaller than the ones that cause dielectric breakdown (Refs. 4 and 15).

[19]E. S. Nylund and G. P. Tsironis (to be published).

[20]H. Engelheart, B. Bullemer, and N. Riehl, in *Physics of Ice*, edited by N. Riehl, B. Bullemer, and H. Engelheart (Plenum, New York, 1969).

[21]The nonmonotonic velocity dependence on temperature is a function of the defect width. This effect should also appear at higher temperatures with wider defects (Ref. 19).